Proc. Natl. Acad. Sci. USA
Vol. 94, pp. 4710–4715, April 1997
Medical Sciences

Ras-dependent pathways induce obstructive hypertrophy in echo-selected transgenic mice

(hypertrophic cardiomyopathy/molecular signaling/gene expression/regulation)

KIM R. GOTTSHALL*†‡, JOHN J. HUNTER*†‡, NOBUAKI TANAKA*, NANCY DALTON*, K. DAVID BECKER*†, JOHN ROSS, JR.*, AND KENNETH R. CHIEN*†§

*Department of Medicine and †Center for Molecular Genetics, University of California at San Diego, La Jolla, CA 92093-0613

Communicated by Helen M. Ranney, Alliance Pharmaceutical Corp., San Diego, CA, March 03, 1997 (received for review August 30, 1996)

ABSTRACT **To overcome the genetic and interindividual variability frequently noted in complex phenotypes, we used echocardiographic selection to develop a substrain of myosin light chain (MLC)–Ras (RAS) transgenic mice with an enhanced ventricular hypertrophic phenotype. These echo-selected mice were then compared with wild-type (WT) animals and a pressure overload hypertrophy model (transverse aortic constriction; TAC). Echocardiography demonstrated increased wall thickness in RAS compared with the other groups. We developed novel miniaturized physiological technology to quantitatively identify *in vivo* intraventricular gradients; increased systolic Doppler velocity was seen in the left ventricle (LV) in 69% of RAS vs. none of WT or TAC. Intracavitary pressure gradients were present in 3 of 10 RAS vs. none of TAC or WT. Passive diastolic LV stiffness was not different among the three groups. Myofibrillar disarray was present in all RAS animals and was significantly more extensive (21.7% area fraction) than in TAC (1.5%) or WT (0.0%). RAS mice had selective induction of natriuretic peptide genes in the LV, a pattern distinct from that induced by pressure overload. Juvenile mortality was significantly increased in the offspring of echo-selected RAS parents. We conclude that adaptation of echocardiography to the mouse permits selection for cardiac phenotypes, and that selectively inbred MLC–Ras transgenic mice faithfully reproduce the molecular, physiological, and pathological features of human hypertrophic cardiomyopathy (HCM). Because previous studies support the concept that hypertrophy in human HCM is secondary to dysfunction created by sarcomeric protein mutations, the current studies suggest that Ras-dependent pathways might play a similar role in forms of human HCM.**

Phenotypic variability is the hallmark of complex genetic traits, such as blood pressure and left ventricular (LV) mass, and the individual genes that contribute to such traits are incompletely known. Genetic dissection of such traits depends upon selective breeding of a genetically tractable species (such as the mouse) based upon a measured physiological parameter. Mice transgenic for a ventricular myosin light chain 2 (MLC2v)–*ras* fusion gene display ventricular hypertrophy and selective diastolic dysfunction in transgenic mice (1), but significant interindividual variability in phenotype was noted, suggesting the presence of modifier genes. To address this issue, we report the utility of echocardiography as a screening tool to select homozygotes with moderate to severe LV hypertrophy for further breeding, and the subsequent development of a substrain of MLC–Ras mice (RAS) with an enhanced phenotype and Doppler ultrasound evidence for velocity/pressure gradients within the LV chamber. Adapting miniaturized transaortic catheterization of the LV to quantitate intraventricular gradients, these RAS mice exhibited features typical of hypertrophic cardiomyopathy (HCM), including echocardiographic LV hypertrophy, increased systolic Doppler velocities in the LV, intraventricular pressure gradients by transaortic catheter, significant myocyte disarray on histological sections, variable myocardial fibrosis, and a selective increase in natriuretic peptide gene expression. Sudden juvenile mortality, in a pattern not previously identified in transgenic mice, was significantly increased in the echo-selected RAS substrain. Finally, a comparison among RAS mice, wild-type (WT) animals, and a pressure-overload hypertrophy model in WT mice (transverse aortic constriction, TAC) demonstrated the obstructive hypertrophy, disarray, selective up-regulation of natriuretic peptide gene expression, and sudden death to be sole features of the RAS mice, and not a feature of generalized hypertrophy *per se*.

MATERIALS AND METHODS

Generation of MLC–Ras Substrain with Enhanced Phenotype. Echocardiographic screening of MLC–Ras transgenic mice [founder line F21 (1), third generation in C57 BL/6J background] was performed in the transgenic animal facility using an Apogee CX (ATL Interspec, Bothell, WA) unit equipped with an ATL 9 MHz annular array transducer using previously described techniques (2). A visual scoring system for hypertrophy (none, mild, moderate, severe) reliably distinguished between homozygotes with $\leq$30% increase in LV weight/body weight ratio compared with historical WT controls (scored as none or mild) and those with $>$30% increase (moderate or severe; data not shown). Animals with comparable degrees of moderate to severe LV hypertrophy (assessed by two observers) were intercrossed, and the progeny which likewise demonstrated moderate to severe hypertrophy formed the study group (RAS).

Echocardiography. For subsequent experiments, WT and TAC mice of comparable age and strain (C57 BL/6J) were compared with RAS. Animals from each group were anesthetized using 100 mg/kg ketamine and 5 mg/kg xylazine i.p. and imaged using equipment described above. Measurements were obtained using previously described techniques (2); the results of two independent observers were averaged. Color flow Doppler measurements were used to identify areas of increased (aliased) velocities in the LV chamber and outflow tract, and these were quantitated using pulsed and/or continuous wave Doppler.

The publication costs of this article were defrayed in part by page charge payment. This article must therefore be hereby marked "*advertisement*" in accordance with 18 U.S.C. §1734 solely to indicate this fact.

0027-8424/97/944710-6$2.00/0
PNAS is available online at **http://www.pnas.org**.

Abbreviations: LV, left ventricular; MLC, myosin light chain; HCM, hypertrophic cardiomyopathy; WT, wild type; TAC, transverse aortic constriction; MHC, myosin heavy chain; GAPDH, glyceraldehyde-3-phosphate dehydrogenase; IVS, interventricular septal thickness; PW, LV posterior wall thickness; BNP, brain natriuretic peptide; ANP, atrial natriuretic peptide.

‡K.R.G. and J.J.H. contributed equally to this work.
§To whom reprint requests should be addressed at: Department of Medicine, 0613-C, University of California at San Diego, 9500 Gilman Drive, La Jolla, CA 92093-0613. e-mail: kchien@ucsd.edu.

Closed Chest Hemodynamics. Immediately following echocardiography, in selected mice the right carotid artery was exposed using a cervical incision as described (3). A bilateral vagotomy was then performed, and a 1.8 F high-fidelity micromanometer-tipped catheter (Millar Instruments, Houston, TX) was inserted into the right carotid artery. The micromanometer catheter was then advanced retrogradely across the aortic valve into the LV and repositioned to obtain a normal LV pressure waveform. The catheter was then withdrawn slowly with continuous recording until the aortic valve was again crossed; this process was repeated twice. Measurements of LV systolic and diastolic pressures as well as the rate of change of pressure (dP/dt) were determined (3). For TAC animals, a fluid-filled flame-stretched PE50 tubing was also attached to a manometer and introduced into the left carotid artery to measure the trans-stenotic pressure gradient, ensuring that adequate pressure-overload was present.

Pressure-Overload Hypertrophy. C57 BL/6J adult mice (Harlan–Sprague–Dawley) were anesthetized using 100 mg/kg ketamine and 5 mg/kg xylazine i.p. and underwent transverse aortic constriction via a mini-thoracotomy in the left third intercostal space as described (3). Animals were allowed to recover; echocardiography and closed chest hemodynamics were performed 1 week after induction of pressure overload, a time at which the hypertrophic response plateaus (3). To control for a potential delay in the development of fibrosis or myocyte disarray, a second group was studied 2 months after aortic constriction.

Morphological Analysis. Hearts were arrested in diastole with a KCl-containing buffer (2) supplemented with adenosine (7.4 μM). For diastolic pressure–volume analysis, the heart was then rapidly excised and a polypropylene membrane balloon (connected to a Statham P23 Db pressure transducer and 100 μl Hamilton syringe) secured in the LV. After determination of the chamber volume at zero pressure (V_0), volume was infused into the balloon in 2.5-μl increments and pressure recorded after recoil, until a pressure of 40 mmHg was reached. Measurements were repeated three times for each heart, and the results averaged. Data from each heart were fitted to a third-order polynomial curve for analysis (4) and were analyzed using both "natural" strain [P vs. $V \times dP/dV$ (5)] and LaGrangian strain [P vs. $(V - V_0)/V_0$)]. Hearts were then fixed with 2% paraformaldehyde and l% glutaraldehyde in PBS at a retrograde aortic pressure of 60 mmHg and a left atrial pressure of 5 mmHg (6).

Quantitative Morphometry. For measurement of disarray, transverse sections of the ventricles were embedded in paraffin and sectioned at 5 μm, stained with hematoxylin/eosin, and visualized on a Nikon Labophot-2 microscope under a $\times$20 objective fitted with a Sony CMA-D1 RGB color camera. Images were acquired on to a Macintosh Quadra 950 computer using COLORKIT (Data Translation, Marlboro, MA) and analyzed using NIH IMAGE (version 1.52). Regions of interest completely covered the circumferentially oriented midwall fibers of the interventricular septum, as described (8). Identification of abnormally arranged cardiac muscle cells was performed as described (7). The area fraction of disarray was expressed as the proportion of the regions of interest occupied by disarrayed myocytes. For analysis of collagen, tissue blocks were cut from the LV free wall parallel to the epicardium and sectioned as above. After staining with picrosirius red, sections were visualized using a $\times$40 objective and transilluminated with either incident light (for determination of total tissue area) or polarized light (with the analyzer polarized at 90 degrees to the incident plane, for determination of birefringent collagen area), using previously described methods (8). Twenty fields were analyzed from each heart, and the results averaged. The area fraction of collagen was expressed as birefringent area/total tissue area.

Gene Expression Analysis. Total RNA was prepared from individual LVs (WT, $n = 7$; TAC, $n = 7$; RAS, $n = 7$) by homogenization with a polytron (Brinkmann) and extracted by RNazol (Cinna/Biotecx Laboratories, Friendswood, TX). Ten micrograms of mRNA from each sample was separated on a 1% agarose formaldehyde gel and transferred to a nylon membrane (Magna NT; Micron Separations, Westboro, MA). Prehybridization and hybridization were performed in aqueous solution (QuikHyb; Stratagene). cDNA probes included a 464-bp fragment of mouse brain natriuretic peptide (BNP) prepared by PCR from heart cDNA using primers spanning the coding region (5′-GAGACAAGGGAGAACACGG-3′, 5′-ACACGGACGTAAGCCTCACT-3′); 3′ end of the rat atrial natriuretic peptide (ANP) cDNA (9); 3′ end of mouse MLC2v cDNA (10); 3′ end of mouse MLC2a cDNA (11); α-skeletal actin, smooth muscle actin, α cardiac actin, and β-myosin heavy chain (MHC) fragments were prepared by PCR from mouse heart cDNA using primers previously described (12). Data from densitometry analysis (Ultroscan LKB; Pharmacia) of the Northern blots were corrected for loading by glyceraldehyde-3-phosphate dehydrogenase (GAPDH; human cDNA probe, ATCC 78105). The normalized value for each was expressed as fold induction over average of corrected WT values for each blot. Loading correction using 28S mRNA was not different than GAPDH.

Statistical Analysis. Comparisons among groups were analyzed by ANOVA, with post-hoc analysis using Scheffe's test. Survival analysis was performed using the log-rank method (Mantel–Haenszel).

RESULTS

Echocardiographic Selection for Enhanced Phenotype. Echocardiography was performed in the transgenic colony on MLC–Ras homozygotes. Of 91 animals screened, 56 had mild or no LV hypertrophy using a visual scoring system, while 35 had moderate to severe hypertrophy (38%). Of the latter group, 13 animals were selected for further breeding, to enrich for more severe hypertrophy within the MLC–Ras genotype. The progeny of these matings were again screened by echocardiography; 25 of 46 animals had moderate to severe hypertrophy (54%), a significant increase from that seen in the initial screening group ($P = 0.02$, χ^2). A group of these animals (RAS) aged 10–14 months was studied further and compared with comparably aged WT (C57BL/6J strain) and WT animals with a surgical model of pressure overload hypertrophy (TAC). Body weights were not different among the three groups (Ras, 30.01 $\pm$ 1.17; WT, 33.03 $\pm$ 1.40; TAC, 32.50 $\pm$ 1.40, mean $\pm$ SE). In a separate experiment, LV weights (corrected for body weight) from a randomly selected group of progeny of echo-selected MLC–Ras homozygote parents (mean 4.88 $\pm$ 0.26 mg/g, $n = 26$) were 19% greater than those from nonselected MLC–Ras homozygotes (mean 4.11 $\pm$ 0.11, $n = 75$, $P = 0.01$ by unpaired t test). In contrast, the mean LV weight/body weight for WT animals is 3.51 $\pm$ 0.05 ($n = 94$).

Noninvasive and Invasive Assessment. On M-mode echocardiography, LV chamber dimensions were not different among the three groups (Table 1), and fractional shortening in the RAS and TAC groups were not significantly different from the WT; there was a statistically significant decrease in the RAS group compared with TAC, but the averages were well within the normal range. Mild concentric hypertrophy was present in the TAC group compared with WT, although this did not reach statistical significance. In the 12 RAS mice (with moderate to severe hypertrophy on screening) that underwent serial echocardiographic and hemodynamic studies, average thickness of both the IVS and the PW were significantly increased; the range for IVS was 0.82–2.22 mm in RAS vs. 0.6–1.0 mm in WT, while corresponding values for PW were 0.82–2.54 mm in RAS vs. 0.5–1.1 mm in WT. Considering a difference between IVS and PW exceeding 0.20 mm significant, in seven RAS mice there was predominant hypertrophy of the PW, in one of the IVS, and in four the degree of hypertrophy was equal. Thus, hypertrophy in the RAS LV may be either concentric or asymmetrical, and when asymmetrical

Table 1. Selected echocardiographic and hemodynamic measurements

	WT		TAC		RAS	
	Mean ± SEM	*n*	Mean ± SEM	*n*	Mean ± SEM	*n*
LVEDD, mm	3.9 ± 0.1	31	3.9 ± 0.2	5	3.9 ± 0.2	12
LVESD, mm	2.3 ± 0.1	31	2.1 ± 0.2	5	2.4 ± 0.2	12
FS, %	41.2 ± 0.1	31	47.1 ± 2.3	5	39.0 ± 2.0†	12
IVS, mm	0.7 ± 0.0	30	0.9 ± 0.0	5	0.9 ± 0.1*	12
PW, mm	0.7 ± 0.0	31	0.8 ± 0.1	5	1.2 ± 0.1*†	12
HR, beats/min	368 ± 24	6	309 ± 43	4	397 ± 19	9
LVESP, mmHg	106.7 ± 4.4	6	101.1 ± 10.0	4	109.8 ± 9.0	9
LVEDP, mmHg	2.3 ± 0.4	6	5.2 ± 1.5	4	5.6 ± 1.1	9
Max dP/dt, mmHg/s	8979 ± 737	6	6328 ± 460	4	8411 ± 695	9
Min dP/dt, mmHg/s	−7,058 ± 308	6	−5,416 ± 179	4	−6,756 ± 479	9

LVEDD, LV end-diastolic dimension; LVESD, LV end-systolic dimension; FS, fractional shortening; IVS, interventricular septal thickness; PW, LV posterior wall thickness; HR, heart rate; LVESP, LV end-systolic pressure; LVEDP, LV end-diastolic pressure; dP/dt, instantaneous rate of change of pressure with respect to time.
*$P < 0.05$ vs. WT; †$P < 0.05$ vs. TAC.

may involve either the IVS or PW, but most commonly the latter. No RAS animal had an IVS/PW ratio >1.5:1. Occasionally, apical hypertrophy has been noted in RAS mice (J.J.H. and N.D., unpublished observations).

Doppler ultrasound failed to demonstrate any increase in systolic velocities in TAC mice compared with WT, either within the LV cavity or in the outflow tract (localized by color flow mapping). In RAS mice systolic velocities in the LV outflow tract or mid-LV exceeding 0.9 m/s were present in 8 of 13 (62%) RAS mice, usually marked by a late-peaking waveform (Fig. 1B). Such a late-peaking signal was present in 36% (14 of 39) of other RAS mice screened and was exclusively associated with moderate-to-severe qualitative hypertrophy. Color Doppler imaging showed aliasing indicative of turbulent flow in the LV outflow tract or mid-cavitary region in 4 of the 13 mice also studied hemodynamically.

Using a new high-fidelity micromanometer tip catheter small enough to pass via the carotid artery and retrogradely cross the aortic valve into the LV of the mouse, it is possible to measure hemodynamics in the closed-chest mouse and to identify the presence of an intraventricular pressure gradient. LV end-systolic pressures, dP/dt_{max} values, and end-diastolic pressures were not different among the three experimental groups (Table 1). No intraventricular pressure gradients were found in any WT or TAC mice. In the 12 RAS mice studied hemodynamically after echocardiography, 3 died before a pullback pressure tracing within the LV could be obtained. In 3 of the 9 remaining animals (30%) an intraventricular pressure gradient was recorded (Fig. 1*A*). All 3 of these animals had an increased Doppler velocity signal (exceeding 0.9 m/s) within the LV, and aliasing of the color-encoded Doppler signal was recorded within the LV in 2 of them, whereas color Doppler imaging was not performed in the third. In all 3 mice, the PW was thicker than the IVS, and either the septal or posterior wall thickness was increased above 0.9 mm [>2SD above normal (2)]. Two others of the 13 RAS mice studied had aliasing on color imaging; in 1 it was associated with no pressure gradient, while the other animal died before a pullback pressure recording was done. The high-velocity jets in the LV together with color aliasing provide good evidence that the pressure gradients recorded by catheter were due to obstruction to outflow, rather than trapping of the catheter in the hypertrophied LV. The observation that some RAS animals with LV cavity obliteration during systole (as observed by echocardiography) had no gradient on catheter pullback also suggests that the observed pressure gradients were due to obstruction within the LV rather than to trapping. Catheter entrapment can be excluded definitively by LV angiography in human subjects with HCM, but this procedure was not available for the mice.

RAS Mice Have Marked Myocyte Disarray But Variable Fibrosis. To determine if the diastolic dysfunction observed in RAS mice was due to alterations in the passive stiffness of the LV chamber, pressure–volume relationships were measured in hearts arrested in diastole. Neither RAS nor TAC animals were significantly different from WT when normalized for chamber size, suggesting that abnormalities in diastolic function are secondary

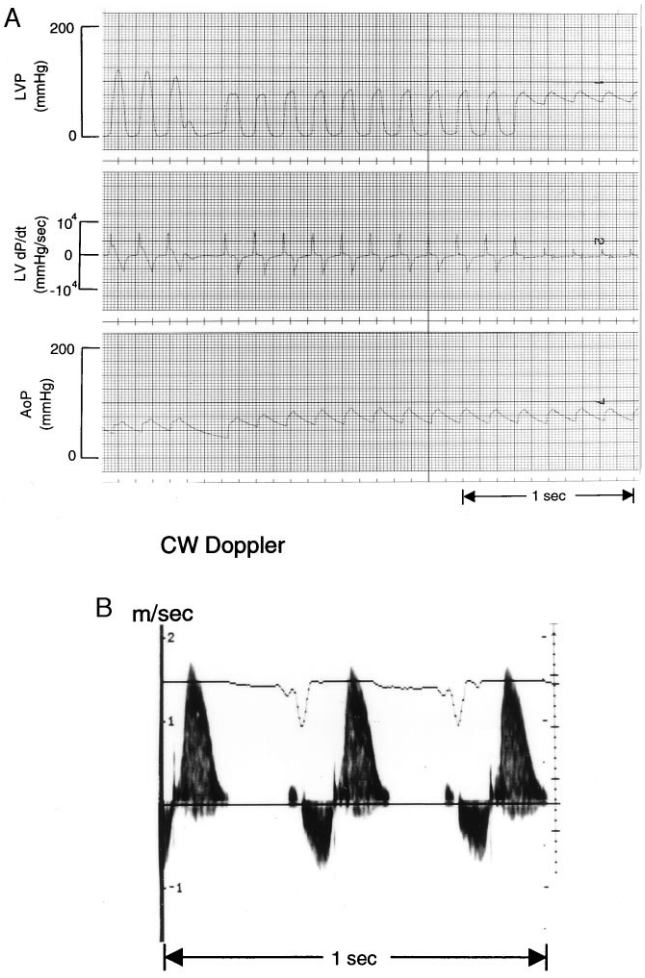

FIG. 1. Intraventricular pressure/velocity gradients. (*A*) Pullback of micromanometer-tip catheter from LV to aorta. A decrease in systolic pressure of 35 mmHg is evident within the LV cavity. LVP, LV pressure. AoP, aortic pressure. (*B*) Doppler ultrasound signal from same animal with sample volume placed in the mid-ventricular region (by color-encoded Doppler signal). Signal below baseline (velocity away from transducer) occurs during systole; that above baseline (velocity toward transducer) occurs during early diastole.

to abnormal active relaxation rather than passive chamber wall properties. Similar findings have been reported in human HCM (13). Using identical methods to those described by Maron and Roberts (7), WT mice exhibited no evidence of disarray (0.0 ± 0.0%, $n = 4$) while TAC mice had minimal disarray (1.5 ± 0.5%, $n = 4$). Aortic constriction for 2 months was not different than the 1-week TAC group (1.3 ± 0.3%, $n = 4$). In contrast, however, RAS mice had 21.7 ± 5.0% disarray (range, 12–30%, $n = 4$), which was statistically significant vs. both other groups [WT and TAC (combined 1 week and 2 month), $P < 0.001$; Fig. 2]. In both extent and range of disarray, RAS mice showed identical findings to HCM in humans, while WT and TAC mice were comparable to normal and diseased human hearts, respectively (7).

Quantitative analysis of the extent of collagen deposition demonstrated a highly variable increase in collagen area fraction in RAS mice compared with the other groups. Average collagen area fraction in RAS was 3.03 ± 2.06%, with a range from a rather normal 0.8% to a striking 9%; other groups were more uniform, with TAC averaging 0.06 ± 0.03% ($n = 8$; 1-week and 2-month TAC groups were not different from each other, and these were combined) and WT averaging 0.01 ± 0.01%. Because of marked variability and fairly small sample size, the differences among groups did not reach statistical significance. The pattern of fibrosis seen in the RAS animals with most extensive fibrosis included both fibrous septae and an increase in perivascular collagen. No systematic comparison of subepicardial and subendocardial regions was performed, nor was the interventricular septum evaluated, although no grossly apparent differences were present among different regions. The technique used relatively low magnification; it is possible that less severe degrees of reactive fibrosis might exist in the TAC as well as RAS hearts.

RAS Mice Selectively Increase ANP and BNP Gene Expression. Gene expression of LV mRNA was analyzed by Northern blot analysis in RAS, TAC, and WT mice (Fig. 3). mRNAs for genes that are not selectively increased during pressure overload hypertrophy, including MLC2v and cardiac α-actin, were not selectively increased in any group (Fig. 3*B*). Moreover, gene isoforms whose mRNA is typically up-regulated by pressure overload hypertrophy, such as skeletal α-actin and β-MHC, were selectively up-regulated in TAC mice (2.9 ± 0.6-fold and 2.6 ± 0.5-fold, respectively) but not in WT or RAS (Fig. 3*C*). Smooth muscle α-actin was not increased in any group, but the atrial isoform of MLC2a was significantly up-regulated in TAC mice, a finding not previously described (Fig. 3*C*). The most dramatic changes in gene expression were seen in the natriuretic peptides, ANP and BNP. As expected,

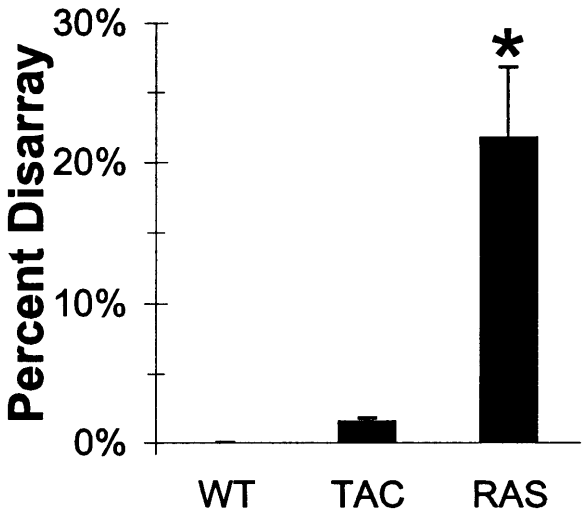

FIG. 2. Quantitative myocyte disarray. Results are shown as area fraction (mean + SEM) of longitudinally oriented myocytes in intraventricular septum that is disarrayed. *, $P < 0.001$ vs. both other groups.

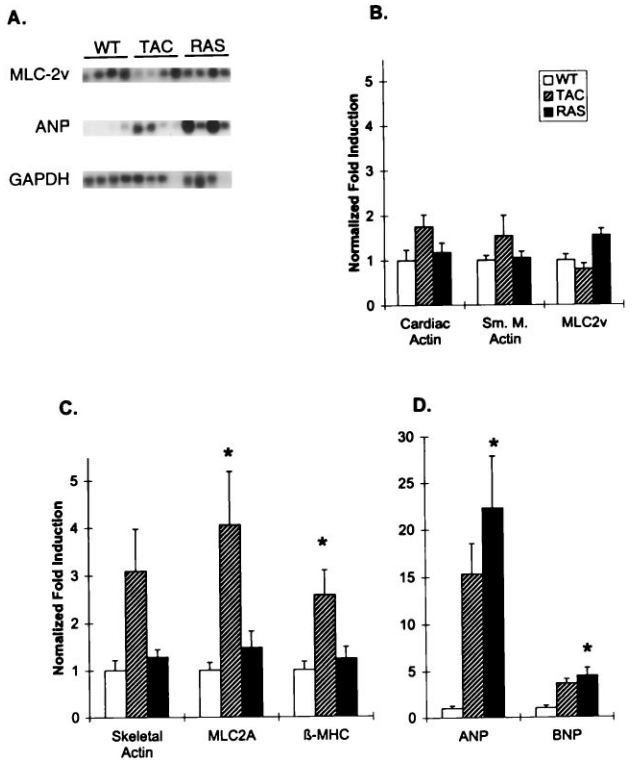

FIG. 3. Northern blot analysis. (*A*) Representative Northern blot showing probes for ANP, MLC2v ($n = 4$), and GAPDH (each lane represents RNA from one animal). (*B*) Fold induction (over WT) of mRNAs for cardiac α-actin ($n = 7, 11, 8$), smooth muscle α-actin ($n = 7, 12, 8$), and MLC2v ($n = 7, 11, 8$) (corrected for differences in loading using GAPDH signal). (*C*) Fold induction of mRNAs for skeletal α-actin ($n = 16, 17, 12$; includes an additional group of animals not analyzed by echocardiography), MLC2a ($n = 7, 7, 7$), and β-MHC ($n = 7, 8, 8$). (*D*) Fold induction of ANP ($n = 11, 8, 7$) and BNP ($n = 7, 7, 7$). Note that n = WT, TAC, and RAS values respectively. Data are mean + SEM; *, $P < 0.05$ vs. WT.

aortic banding increased ANP and BNP (15.3 ± 3.2-fold and 3.6 ± 0.5-fold, respectively), but this did not reach statistical significance due to high interindividual variability. Unlike the other genes evaluated, ANP and BNP were strongly up-regulated in RAS mice (22.3 ± 5.6-fold and 4.4 ± 0.8-fold, $P < 0.01$ vs. WT, Fig. 3 *A* and *D*). Therefore, RAS transgenic mice display selectivity in their activation of the components of the embryonic gene program, although they may (and likely do) also have a generalized increase in gene expression accompanying the cardiac growth.

Juvenile Mortality. As seen in Fig. 4, survival in the juvenile offspring of echo-selected RAS animals (12 litters) was significantly reduced compared with that for RAS heterozygotes (31 litters) using log-rank survival analysis ($P < 0.001$). The predominant mortality occurred within 1 week of weaning/maturity (14–28 days after birth). Using RAS heterozygotes as a control minimizes the possibility of selection for an unrelated lethal gene cosegregating with the MLC–Ras transgene. Survival of offspring from matings between unselected RAS homozygotes, as well as between RAS heterozygotes and WT animals of an unrelated strain (DBA/2), was not different than that for RAS heterozygote matings (data not shown).

DISCUSSION

Utility of Echocardiographic Selection for Complex *in Vivo* Cardiac Phenotypes in Genetically Manipulated Mice. Creation of a substrain of MLC–Ras transgenic mice, using echocardiography to select for animals with moderate to severe degrees of hypertrophy for further mating, represents a novel method to enrich for a specific cardiac phenotype. By screening successive generations of animals using predeter-

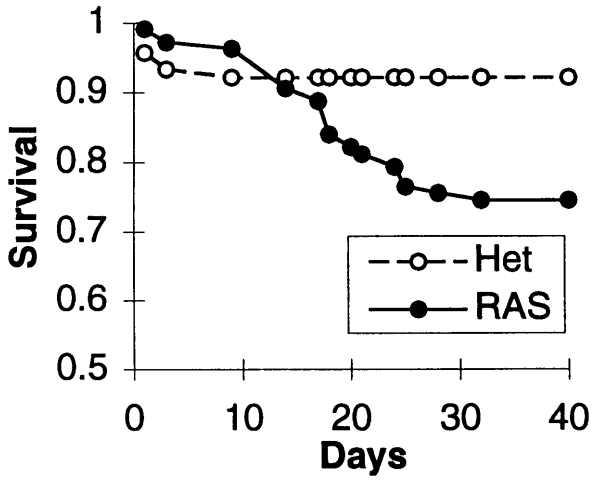

FIG. 4. Survival analysis. RAS, matings between homozygotes of echocardiographically selected substrain of MLC–Ras; Het, matings between unselected MLC–Ras heterozygotes. The survival curves are significantly different ($P < 0.001$).

mined criteria, substrains can be generated with different characteristics, permitting identification of modifier genes through molecular genetic techniques. The adaptation of echocardiographic techniques to the mouse has been demonstrated recently (2, 14–16), and the utility of echocardiography in defining a phenotype of dilated cardiomyopathy has been recently described (17). In the current work, the selected substrain demonstrated features of human HCM much more striking than those seen in the original strain. This raises the possibility that complex cardiac phenotypes may be dissected into groups of component characteristics, with each group reflecting the activity of a common cellular pathway.

Echocardiographic and Hemodynamic Features of Obstructive Hypertrophy Are Present in RAS Mice. Human HCM in symptomatic individuals commonly displays asymmetrical septal hypertrophy (18), but documentation of complete pedigrees in humans (19) reveals great variability in the location, symmetry, and extent of hypertrophy within the genetically affected family members of symptomatic patients. While not reporting the prevalence of asymmetrical hypertrophy, a recent report of a murine model expressing mutant α-MHC identified at least one transgenic animal with posterior wall hypertrophy and sudden death after exercise (20). Most patients with HCM do not have dynamic intracavitary obstruction, but when present it is most often seen in the LV outflow tract; in the presence of asymmetrical septal hypertrophy, such obstruction is associated with an abnormally anterior position of the mitral valve, the mitral apparatus meeting the interventricular septum during systole to form the obstruction as documented angiographically (21) and by echocardiography (22), with a high velocity jet located at that site by Doppler echocardiography (23). The MLC–Ras substrain contained individuals with both symmetrical and asymmetrical LV hypertrophy, with a late-peaking high velocity Doppler jet in the mid LV or outflow tract. When asymmetrical hypertrophy occurred, it most often involved the posterior wall, whereas asymmetrical hypertrophy in humans usually affects most prominently the interventricular septum (24, 25). It is possible that other genetic or species-specific factors may be involved in the determination of the distribution of hypertrophy.

Using a new high-fidelity micromanometer tip catheter small enough to retrogradely cross the aortic valve of the mouse, it is now possible to both measure closed-chest hemodynamics and identify the presence of intraventricular pressure gradients. This technique demonstrated such a gradient in 30% of the echo-selected MLC–Ras substrain. The concurrent presence of a late-peaking high velocity Doppler ultrasound jet within the LV, with turbulent flow (color aliasing) in most RAS mice, further supports the likelihood that the measured pressure gradient usually represented obstruction rather than catheter trapping (26). Color aliasing by echocardiography was difficult to localize precisely because of the small size of the LV chamber in the mouse; nonetheless, it was clearly at the mid-ventricular level in one of the two mice in which this phenomenon was documented by both Doppler ultrasound and an intraventricular pressure gradient on catheter pullback. These echocardiographic and hemodynamic findings resemble those in a minority of patients with HCM who exhibit mid-cavitary LV obstruction with a pressure gradient at that site, associated with a late-peaking high velocity Doppler jet in the mid-LV or outflow tract (27, 28), similar to the findings shown in Fig. 1. This flow pattern also has been reported in some patients without asymmetrical septal hypertrophy who have severe concentric LV hypertrophy, but pressure gradients were not assessed (29); because these patients had predominantly hypertensive LV hypertrophy, it is possible that the phenomenon of mid-cavitary obstruction is related to the severity of hypertrophy. The mid-ventricular obstructive variant of human HCM has recently been associated with mutations in MLCs, both the essential light chain (MLC1) and the regulatory light chain (MLC2) (30). The demonstration of obstruction in a minority of MLC–Ras transgenic mice correlated well with the prevalence of obstruction in human HCM. Thus, these studies document the utility of both Doppler echocardiography and closed-chest, retrograde transaortic LV catheterization in the assessment of cardiac disease in the mouse.

RAS Mice Display Typical Morphological Features of Human HCM. Diastolic dysfunction with preserved or supernormal systolic function is the most common hemodynamic and echocardiographic finding in human HCM. There was no significant difference in the passive stiffness of the LV chamber between RAS mice and normal or pressure-overloaded animals when normalized for chamber size, suggesting that abnormalities in diastolic function are secondary to abnormal active relaxation rather than passive chamber wall properties, as has been reported for humans with HCM (13). Passive chamber properties cannot be excluded from contributing to the final phenotype, since some individuals demonstrated marked stiffness while others fell within the normal range.

Histologically, the hallmark of human HCM is myocyte disarray, which is quantitatively increased compared with other forms of hypertrophic heart disease (7). Using detailed morphological criteria for muscle cell disorganization, 94% of patients with HCM exhibited myofibrillar disarray (89% had area fractions of disarray >5%, and 56% had >25%). Only 7% of hearts from normal individuals or patients with various forms of heart disease exhibited as much as 5% disarray, and none was greater than 10% (7). Applying this methodology to murine models of hypertrophy, we have demonstrated a striking similarity between the findings in RAS mice and humans with HCM; the validity of this approach is supported by the similar extent of disarray in the pressure-overloaded mouse heart and the hypertrophied human heart. It is intriguing that a longer duration of pressure overload did not affect the prevalence of disarray in the mouse. Because the hypertrophic remodeling of the mouse heart in response to pressure overload (as indicated by chamber weight) is largely complete within 1 week in the mouse (3), this suggests that disarray of myocytes is an epiphenomenon of this hypertrophic process that occurs concurrently with cellular growth. Myocyte hypertrophy with qualitative disarray has also been shown in a murine model which expresses an HCM mutation in the α-MHC; interestingly, this transgenic line does not display an increase in LV mass, confirming that disarray is directly related to the hypertrophic process at the cellular level. Assessment of myofibrillar disarray within individual myocytes, using electron microscopy, has not been performed in RAS or TAC mice.

Patients with HCM have an increase in fibrosis in the LV free wall (7.7%, compared with 1.1% in normals). There is a wide variation in the extent of fibrosis in these patients with

HCM (95% confidence intervals 0–16.1%). Fibrosis in the MLC–RAS mice mimics the fibrosis found in humans with HCM, and has also been seen in transgenic mice expressing mutant α-MHC (20). The mechanism by which myocyte hypertrophy produces fibrosis remains to be elucidated.

Selective Induction of Natriuretic Peptide Genes Is Unique to RAS Hypertrophy. Increased cardiac mass in the MLC–Ras substrain is not accompanied by activation of the full complement of embryonic gene isoforms previously identified in pressure-overload hypertrophy in rodents. Although an increase in overall gene expression is anticipated in any growth model, MLC–Ras mice display a striking selective up-regulation of mRNA for the natriuretic peptides ANP and BNP. Up-regulation of the natriuretic peptides has been documented in LV biopsy samples from humans with HCM (31, 32), and plasma levels of ANP are increased in HCM patients (32). Whether induction of natriuretic peptide genes in HCM is also selective among embryonic gene isoforms up-regulated by pressure overload in humans has not yet been assessed. The findings presented above raise the possibility that activation of the natriuretic peptide genes in human HCM and in other hypertrophic heart diseases such as congestive heart failure may involve Ras-dependent pathways.

Offspring of Echocardiographically Selected RAS Mice Have Increased Juvenile Mortality. Sudden death is the most devastating complication of human HCM. Deaths in the offspring of the MLC–Ras echo-selected parents were all of a "sudden" nature without prior signs of distress. Sudden death in adolescence and early adulthood is characteristic of the more severe forms of human HCM, and the mechanisms are not yet identified. There are no data thus far regarding incidence or severity of arrhythmias in MLC–Ras mice, and the mechanism of death will be the subject of future investigation. This transgenic line, however, is to our knowledge the first model that may provide insight into the cellular and molecular mechanisms of sudden death.

Summary. We have demonstrated the feasibility of using echocardiography in the mouse to identify a specific cardiac phenotype within a transgenic line, and to create a novel substrain that manifests functional, morphological, and molecular features strikingly similar to human HCM. HCM in humans is both phenotypically and genetically heterogeneous; multiple mutations in several sarcomeric protein genes have been identified, and the extent of LV hypertrophy, as well as other diagnostic features of HCM, varies greatly among affected individuals. This suggests that multiple genetic mutations converge on a common pathway to generate a clinically similar spectrum of heart disease. The MLC–Ras transgenic substrain selected by echocardiography manifested intraventricular pressure gradients suggestive of obstruction, similar to human HCM, demonstrated by adaptation of Doppler echocardiography and closed-chest transaortic catheterization techniques used in humans to the mouse. In addition to previously documented diastolic dysfunction, sudden death occurs in late juvenile/early adult animals in the selected substrain of MLC–Ras transgenic mice but not in the parental strain, demonstrating that use of echocardiography as a selection tool can enrich for novel, unsuspected phenotypes. Asymmetrical LV septal hypertrophy, a common finding in human HCM, is not common in the MLC–Ras substrain; however, this is not universally seen in HCM either, and the location of hypertrophy in this disorder may reflect input from other (as-yet unidentified) genes. These findings lead to the hypothesis that the multiple genetic mutations seen in sarcomeric proteins may each induce subtle abnormalities in the contractile function of individual myocytes (33), although sarcomeric assembly is not affected (34). Such mild contractile dysfunction may then (via unknown growth signals) converge on Ras-dependent signaling pathways to produce exaggerated hypertrophy in which overall systolic function is preserved but diastolic dysfunction is initially prominent; this hypertrophic response is characterized by myocyte disarray, variable intracavitary obstruction, patchy fibrosis, and sudden cardiac death. MLC–Ras transgenic mice thus represent a useful model for HCM, which can be used to further elucidate molecular mechanisms underlying various features of the disease, to assess genetic determinants of prognosis, to find and test new modalities of therapy, and to better understand the hypertrophic process itself; the latter has broad implications for many diseases in which cardiac hypertrophy features prominently in adaptation and prognosis, such as hypertensive heart disease, valvular heart disease, and heart failure from many causes.

We are grateful to Dr. Minoru Hongo for his help with diastolic pressure–volume analysis and analysis of echocardiograms. This work was supported by a Training Grant from the National Institutes of Health and the National Eye Institute (K.R.G.); Clinical Investigator Award HL03211 from the National Heart, Lung, and Blood Institute (J.J.H.); an individual National Research Scholar Award from the National Institutes of Health (K.D.B.); National Institutes of Health Grant HL53773 and a chair from the San Diego Affiliate of the American Heart Association (J.R.); as well as National Heart, Lung, and Blood Institute Grants HL53773, HL51549, and HL55926 (K.R.C.).

1. Hunter, J. J., Tanaka, N., Rockman, H. A., Ross, J. & Chien, K. R. (1995) *J. Biol. Chem.* **270,** 23173–23178.
2. Tanaka, N., Dalton, N., Mao, L., Rockman, H. A., Peterson, K. L., Gottshall, K. R., Hunter, J. J., Chien, K. R. & Ross, J., Jr. (1996) *Circulation* **94,** 1109–1117.
3. Rockman, H. A., Knowlton, K. U., Ross, J., Jr., Chien, K. R. (1993) *Circulation* **87,** Suppl VII, VII-1–VII-21.
4. Omens, J. H., Rockman, H. A. & Covell, J. W. (1994) *Am. J. Physiol.* **266,** H1169–H1176.
5. Mirsky, I. (1984) *Circulation* **69,** 836–841.
6. Duerr, R. L., Huang, S., Miraliakbar, H. R., Clark, R., Chien, K. R. & Ross, J., Jr. (1995) *J. Clin. Invest.* **95,** 619–627.
7. Maron, B. J. & Roberts, W. C. (1979) *Circulation* **59,** 689–706.
8. Omens, J. H., Milkes, D. E. & Covell, J. W. (1995) *Ann. Biomed. Eng.* **23,** 152–163.
9. Knowlton, K. U., Barracchini, E., Ross, R. S., Harris, A. N. & Henderson, S. A., Evans, S. M., Glembotski, C. C., Chien, K. R. (1991) *J. Biol. Chem.* **266,** 7759–7768.
10. Lee, K. J., Ross, R. S., Rockman, H. A., Harris, A. N., O'Brien, T. X., van Bilsen, M., Shubeita, H. E., Kandolf, R., Brem, G., Price, J., Evans, S. M., Zhu, H., Franz, W. M. & Chien, K. R. (1992) *J. Biol. Chem.* **267,** 15875–15885.
11. Kubalak, S. W., Miller-Hance, W. C., O'Brien, T. X., Dyson, E. & Chien, K. R. (1994) *J. Biol. Chem.* **269,** 16961–16970.
12. Miller-Hance, W. C., LaCorbiere, M., Fuller, S. J., Evans, S. M., Lyons, G., Schmidt, C., Robbins, J. & Chien, K. R. (1993) *J. Biol. Chem.* **268,** 25244–25252.
13. Pak, P. H., Maughan, W. L., Baughman, K. L. & Kass, D. A. (1996) *Circulation* **94,** 52–60.
14. Manning, W. J., Wei, J. Y., Katz, S. E., Litwin, S. E. & Douglas, P. S. (1994) *Am. J. Physiol.* **266,** H1672–H1675.
15. Gardin, J. M., Siri, R. M., Kitsis, R. N., Edwards, J. G. & Leinwand, L. A. (1995) *Circ. Res.* **76,** 907–914.
16. Hoit, B. D., Khory, S. F., Kranias, E. G., Ball, N. & Walsh, R. A. (1995) *Circ. Res.* **77,** 632–637.
17. Arber, S., Hunter, J. J., Ross, J., Jr., Hongo, M., Sansig, G., Borg, J., Perriard, J.-C., Chien, K. R. & Caroni, P. (1997) *Cell* **88,** 393–403.
18. Henry, W. L., Clark, C. E. & Epstein, S. E. (1973) *Circulation* **47,** 225–233.
19. Fananapazir, L. & Epstein, N. D. (1994) *Circulation* **89,** 22–32.
20. Geisterfer-Lowrance, A. A. T., Christe, M., Conner, D. A., Ingwall, J. S., Schoen, F. J., Seidman, C. E. & Seidman, J. G. (1996) *Science* **272,** 731–734.
21. Ross, J. Jr., Braunwald, E., Gault, J. H., Mason, D. T. & Morrow, A. G. (1966) *Circulation* **34,** 558–578.
22. Shah, P. M., Taylor, R. D. & Wong, M. (1981) *Am. J. Cardiol.* **48,** 258–262.
23. Maron, B. J., Gottdiener, J. S., Arce, J., Rosing, D. R., Wesley, Y. E. & Epstein, S. E. (1985) *J. Am. Coll. Cardiol.* **6,** 1–15.
24. Maron, B. J., Gottdiener, J. S. & Epstein, S. E. (1981) *Am. J. Cardiol.* **48,** 418–428.
25. Gilbert, B. W., Pollick, C., Adelman, A. G. & Wigle, E. D. (1980) *Am. J. Cardiol.* **45,** 861–872.
26. Levine, R. A. & Weyman, A. E. (1985) *J. Am. Coll. Cardiol.* **6,** 16–18.
27. Falicov, R. E., Resnekov, L., Bharati, S. & Lev, M. (1976) *Am. J. Cardiol.* **37,** 432–4437.
28. Schwammenthal, E., Block, M., Schwartzkopff, B., Lösse, B., Borggrefe, M., Schulte, H. D., Bircks, W. & Breithardt, G. (1992) *J. Am. Coll. Cardiol.* **20,** 964–973.
29. Harrison, M. R., Grigsby, C. G., Souther, S. K., Smith, M. K. & DeMaria, A. N. (1991) *Am. J. Cardiol.* **68,** 761–765.
30. Poetter, K., Jiang, H., Hassanzadeh, S., Master, S. R., Chang, A., Dalakas, M. C., Rayment, I., Sellers, J. R., Fananapazir, L. & Epstein, N. D. (1996) *Nat. Genet.* **13,** 63–69.
31. Takemura, G., Fujiwara, H., Mukoyama, M., Saito, Y., Nakao, K., Kawamura, A., Ishida, M., Kida, M., Uegaito, T., Tanaka, M., Matsumori, A., Fujiwara, T., Imura, H. & Kawai, C. (1991) *Circulation* **83,** 181–190.
32. Hasegawa, K., Fujiwara, H., Doyama, K., Miyamae, M., Fujiwara, T., Suga, S., Mukoyama, M., Nakao, K., Imura, H. & Sasayama, S. (1993) *Circulation* **88,** 372–380.
33. Watkins, H., Seidman, C. E., Seidman, J. G., Feng, H. S. & Sweeney, H. L. (1996) *J. Clin. Invest.* **98,** 2456–2461.
34. Becker, K. D., Gottshall, K. R., Hickey, R., Perriard, J.-C. & Chien, K. R. (1997) *J. Cell Biol.* **137,** 131–140.